Journal of Solid State Chemistry 182 (2009) 2497–2509

Contents lists available at ScienceDirect

Journal of Solid State Chemistry

journal homepage: www.elsevier.com/locate/jssc

The ternary system cerium–palladium–silicon

Alexey Lipatov [a,b], Alexander Gribanov [a,c], Andriy Grytsiv [a], Peter Rogl [a,*], Elena Murashova [c], Yurii Seropegin [c], Gerald Giester [d], Konstantin Kalmykov [c]

[a] Institute of Physical Chemistry, University of Vienna, Währingerstrasse 42, A-1090 Wien, Austria
[b] Materials Science Department of the Moscow State University, Leninskie Gory, GSP-1, 119991 Moscow, Russia
[c] Chemistry Department of the Moscow State University, Leninskie Gory, GSP-1, 119991 Moscow, Russia
[d] Institute of Mineralogy and Crystallography, University of Vienna, Althanstrasse 14, A-1090 Wien, Austria

ARTICLE INFO

Article history:
Received 15 March 2009
Received in revised form
8 June 2009
Accepted 13 June 2009
Available online 21 June 2009

Keywords:
Ternary system Ce–Pd–Si
Ternary silicides
Phase equilibria at 800 °C
X-ray single crystal and powder diffraction

ABSTRACT

Phase relations in the ternary system Ce–Pd–Si have been established for the isothermal section at 800 °C based on X-ray powder diffraction and EMPA techniques on about 130 alloys, which were prepared by arc-melting under argon or powder reaction sintering. Eighteen ternary compounds have been observed to participate in the phase equilibria at 800 °C. Atom order was determined by direct methods from X-ray single-crystal counter data for the crystal structures of τ_8—$Ce_3Pd_4Si_4$ ($U_3Ni_4Si_4$-type, *Immm*; $a = 0.41618(1)$, $b = 0.42640(1)$, $c = 2.45744(7)$ nm), τ_{16}—$Ce_2Pd_{14}Si$ (own structure type, *P4/nmm*; $a = 0.88832(2)$, $c = 0.69600(2)$ nm) and also for τ_{18}—$CePd_{1-x}Si_x$ ($x = 0.07$; FeB-type, *Pnma*; $a = 0.74422(5)$, $b = 0.45548(3)$, $c = 0.58569(4)$ nm). Rietveld refinements established the atom arrangement in the structures of τ_5—Ce_3PdSi_3 ($Ba_3Al_2Ge_2$-type, *Immm*; $a = 0.41207(1)$, $b = 0.43026(1)$, $c = 1.84069(4)$ nm) and τ_{13}—$Ce_{3-x}Pd_{20+x}Si_6$ ($0 \le x \le 1$, $Co_{20}Al_3B_6$-type, $Fm\bar{3}m$; $a = 1.21527(2)$ nm). The ternary compound $Ce_2Pd_3Si_3$ (structure-type $Ce_2Rh_{1.35}Ge_{4.65}$, *Pmmn*; $a = 0.42040(1)$, $b = 0.42247(1)$, $c = 1.72444(3)$ nm) was detected as a high-temperature compound, however, does not participate in the equilibria at 800 °C. Phase equilibria in Ce–Pd–Si are characterized by the absence of cerium solubility in palladium silicides. Mutual solubility among cerium silicides and cerium–palladium compounds are significant whereby random substitution of the almost equally sized atom species palladium and silicon is reflected in extended homogeneous regions at constant Ce-content such as for τ_2—$Ce(Pd_xSi_{1-x})_2$ (AlB_2-derivative type), τ_6—$Ce(Pd_xSi_{1-x})_2$ ($ThSi_2$-type) and τ_7—$CePd_{2-x}Si_{2+x}$. The crystal structures of compounds τ_4—$Ce_{\sim 8}Pd_{\sim 46}Si_{\sim 46}$, τ_{12}—$Ce_{\sim 29}Pd_{\sim 49}Si_{\sim 22}$, τ_{15}—$Ce_{\sim 22}Pd_{\sim 67}Si_{\sim 11}$, τ_{17}—$Ce_{\sim 5}Pd_{\sim 77}Si_{\sim 18}$ and τ_{18}—$CePd_{1-x}Si_x$ ($x \sim 0.1$) are still unknown.

1. Introduction

Investigation of Ce–Pd–Si alloys was mainly driven by the search for novel compounds with interesting electrical and/or magnetic properties such as heavy-fermion materials and/or Kondo-lattice compounds, some of which have already been characterized e.g. $Ce_2Pd_3Si_5$, Ce_2PdSi_3, $Ce_3Pd_{20}Si_6$, $CePd_2Si$ and $CePd_2Si_2$ [1]. A recent critical assessment [1] summarized all data available then on the Ce–Pd–Si system essentially based on phase equilibria derived for an isothermal section at 600 °C by Seropegin et al. [2]. As a result of the critical review an isothermal section at 600 °C was presented, which, however, left many regions in the diagram open for further studies. The present paper attempts to fill these gaps i.e. to provide a comprehensive knowledge on the phase equilibria and crystal structures in the Ce–Pd–Si ternary system. In order to profit from enhanced diffusion in the system combining elements with rather different melting points, a temperature of 800 °C was chosen for the isothermal section.

2. Experimental techniques

More than 130 alloys, each with a weight of 1 g, were prepared by argon arc-melting from high-purity elements (>99.9 mass%), on a water-cooled copper hearth. To ensure homogenization, all alloys were re-melted three times. Part of each sample was vacuum-sealed in quartz tubes and annealed at 800 °C for 15–30 days before being quenched in cold water. Alloys, which even after long-term anneal did not reach equilibrium were powderized, cold compacted and sintered at 800 °C for 2 weeks.

X-ray powder diffraction (XRD) data from as-cast and annealed alloys were collected from a Guinier–Huber image plate system (Cu$K\alpha_1$; $8° < 2\theta < 100°$) and/or an STOE STADI P transmission diffractometer, equipped with a linear PSD (Cu$K\alpha_1$-radiation; $10° < 2\theta < 90°$). Precise lattice parameters were calibrated against

* Corresponding author. Fax: +43 1 4277 9524.
E-mail address: peter.franz.rogl@univie.ac.at (P. Rogl).

0022-4596/$ - see front matter © 2009 Elsevier Inc. All rights reserved.
doi:10.1016/j.jssc.2009.06.022

Table 1
Crystallographic data of solid phases in the Ce–Pd–Si system.

Phase	Space group	Lattice parameters (nm)			Comments
Temperature range (°C)	Prototype	*a*	*b*	*c*	
(δ-Ce)	$Im\bar{3}m$	0.412			[34]
789–726 [34]	W				
(γ-Ce)	$Fm\bar{3}m$	0.51610			[34]
726–61 [34]	Cu				
(β-Ce)	$P6_3/mmc$	0.36810		1.1857	[34]
61–(−177) [34]	α-La				
(α-Ce)	$Fm\bar{3}m$	0.485			[34]
<−177 [34]	Cu				
(Pd)	$Fm\bar{3}m$	0.38903			[34]
<1555 [34]	Cu				
(Si)	$Fm\bar{3}m$	0.54306			[34]
<1414 [34]	C (diamond)				
Ce_5Si_3	$I4/mcm$	0.7868		1.373	[35]
<1260 [11]	Cr_5B_3	0.7878		1.367	[11]
$Ce_5(Pd_xSi_{1-x})_3$					$0 \le x \le 0.14$ (this work)
		0.78632 (5)		1.3816 (1)	$x = 0.11$ (this work)
		0.78563 (2)		1.3825 (1)	$x_{max} = 0.14$ (this work)
Ce_3Si_2	$P4/mbm$	0.7780		0.4367	[11]
<1335 [11]	U_3Si_2				
$Ce_3(Pd_xSi_{1-x})_2$					$0 \le x \le 0.10$ (this work)
		0.78021 (5)		0.43627 (3)	$x = 0.07$ (this work)
		0.77992 (1)		0.43656 (1)	$x_{max} = 0.10$ (this work)
Ce_5Si_4	$P4_12_12$	0.7936		1.5029	[11]
<1500 [11]	Zr_5Si_4				
$Ce_5(Pd_xSi_{1-x})_4$					$0 \le x \le 0.16$ (this work)
		0.79574 (5)		1.5006 (3)	$x = 0.10$ (this work)
		0.79636 (6)		1.4979 (2)	$x = 0.12$ (this work)
		0.79678 (6)		1.4937 (2)	$x_{max} = 0.16$ (this work)
CeSi	*Pnma*	0.8298	0.3961	0.5959	[11]
<1630 [11]	FeB	0.83035 (7)	0.39651 (4)	0.59623 (5)	(this work)
$CeSi_{1-x}Pd_x$		0.82880 (6)	0.39803 (4)	0.59593 (6)	$x_{max} = 0.02$ (this work)
Ce_2Si_{3-x}	*Cmcm*				$x = 0.32$ [12]
	V_2B_3	0.44035	2.48389	0.39517	at 35 K [12]
$CeSi_{1.67}$	*Imma*	0.4109	0.4189	1.3917	at 62.6 at% Si [11]
<1725 [11]	$GdSi_{2-x}$				
$CeSi_{2-x}$	$I4_1/amd$	–	–	–	$0 \le x \le 0.21$ [11]
<1575 [11]	$ThSi_2$	0.4192		1.3913	$x = 0$ [11]
		0.41897 (3)		1.3932 (1)	$x = 0$ (this work)
$Ce(Pd_ySi_{1-y})_{2-x}$					$0 \le y \le 0.188$ (this work)
		0.4189		1.4241	$x = 0$, $y = 0.2$ [24]
		0.42016 (1)		1.4008 (1)	$x = 0$, $y = 0.075$ (this work)
		0.41968 (1)		1.4140 (1)	$x = 0$, $y = 0.15$ (this work)
		0.41897 (1)		1.4202 (1)	$x = 0$, $y_{max} = 0.188$ (this work)
Ce_7Pd_3	$P6_3mc$	1.0222		0.6441	[36]
$Ce_7(Pd_{1-x}Si_x)_3$	Th_7Fe_3				
Ce_3Pd_2	Unknown				[36]
α-CePd	*Cmcm*	0.3890	1.0910	0.4635	[21]
<1005 [16]	CrB	0.38893 (2)	1.0932 (1)	0.46229 (5)	(this work)
β-CePd		–	–	–	[21]
1130–1005 [16]					
$CePd_{1-x}Si_x$	*Pnma*	0.74422 (5)	0.45548 (3)	0.58569 (4)	$x = 0.07$, SC data, (this work)
	FeB				
Ce_3Pd_4	$R\bar{3}$	1.3669		0.5824	[36]
≤1130 [16]	Pu_3Pd_4	1.3699 (2)		0.5813 (1)	(this work)
Ce_3Pd_5	$P\bar{6}2m$	0.725		0.385	[18]
≤1037 [16]	Th_3Pd_5				
	Unknown				[19], (this work)
$CePd_{3+x}$	$Pm\bar{3}m$				$-0.002 \le x \le 0.012$ [37]
≤1437 [16]	Cu_3Au	0.4129			$x = 0$ [19]
		0.4112			$x = 0.01$ [19]
		0.4160			[35]
		0.41307 (1)			$x = 0.004$ (this work)
$Ce(Pd_{1-y}Si_y)_{3+x}$					$0 \le y \le 0.08$ (this work)
		0.4194			$CePd_3Si_{0.15}$ [38]
		0.41582 (1)			$x = 0$, $y = 0.02$ (this work)
		0.42422 (3)			$x = 0$, $y_{max} = 0.08$ (this work)
α-$CePd_5$	c^*	0.4038			[39]
≤801 [40]		0.4055			[17]
1060–1348 [17]		0.40283 (1)			(this work)
$Ce(Pd_{1-x}Si_x)_5$		0.41307 (1)			$x_{max} = 0.048$ (this work)
	Pnma	0.57004	0.40622	0.84617	[41]
	α-$CePd_5$				

Table 1 (*continued*)

Phase	Space group	Lattice parameters (nm)			Comments
Temperature range (°C)	Prototype	*a*	*b*	*c*	
β-$CePd_5$	P6/*mmm*	0.5373		0.4177	[42]
801–1180 [40]	$CaCu_5$				
α-$Ce_{1-x}Pd_{7+x}$	*h***				$-0.016 \le x \le 0.168$ at 550 °C [17]
≤709 [40]		0.25930		0.41679	$x = -0.016$ [17]
		0.25960		0.40483	$x = 0.168$ [17]
β-$Ce_{1-x}Pd_{7+x}$	$Fm\bar{3}m$				$-0.024 \le x \le 0.184$ at 1000 °C [17]
709–1543 [17]	$CuPt_7$	0.8125			$x = -0.024$ [17]
		0.7955			$x = 0.184$ [17]
		0.7946 (1)			$x = 0.23$ (this work)
		0.7986 (1)			$x = -0.008$ (this work)
$Pd_{84-x}Si_{16+x}$	Unknown				$0 \le x \le 0.3$ [15]
< 811 [15]					
Pd_5Si	$P2_1$	0.5555	0.7485	0.8465	[43]
856–811 [15]	Pd_5P		$\beta = 100.7°$		
$Pd_{14}Si_3$	Unknown				[44]
<795 [15]					
Pd_9Si_2	*Pnma*	0.90548	0.74188	0.94014	[43]
819–764 [15]	Pd_9Si_2	0.9052 (1)	0.7417 (1)	0.9401 (1)	(this work)
$Pd_{15}Si_4$	$P\bar{1}$	0.4402	0.7700	0.8990	[45]
792–753 [15]		$\alpha = 111.02°$	$\beta = 96.52°$	$\gamma = 89.15°$	
Pd_3Si	*Pnma*	0.5735	0.7553	0.5260	[43]
<1064 [15]	Fe_3C	0.5737 (1)	0.7556 (2)	0.5263 (1)	(this work)
Pd_2Si (1)	Unknown				33.3 at% Si [15]
<1053 [15]					
Pd_2Si (2)		–	–	–	33.5 at% Si [15]
<1404 [15]	$P\bar{6}2m$	0.6496		0.3433	[46]
	Fe_2P	0.6502 (1)		0.3432 (1)	(this work)
Pd_2Si (3)	Unknown				33.9 at% Si [15]
<1080 [15]					
Pd_2Si (4)	Unknown				34.5 at% Si [15]
<1072 [15]					
PdSi	*Pnma*	0.5599	0.3381	0.6133	[47]
908–888 [15]	MnP	0.56116 (3)	0.33867 (2)	0.61476 (2)	(this work)
865–824 [44]					
τ_1, $CePdSi_3$	*I*4*mm*	0.4330		0.9631	[24]
	$BaNiSn_3$	0.43209		0.9606	[2]
		0.43189 (2)		0.96061 (8)	(this work)
τ_2, $Ce(Pd_xSi_{1-x})_2$	P6/*mmm*	0.4129		0.4285	$x = 0.25$ [24]
	AlB_2[b]	0.4121		0.4272	$x = 0.25$ [48]
		0.4134		0.4219	$x = 0.3$ [2]
		0.41325		0.42684	$x = 0.2$ [49]
	AlB_2-				$0.215 \le x \le 0.321$ (this work)
	derivative	0.41131 (2)		0.42820 (2)	$x_{min} = 0.215$ (this work)[c]
		0.41174 (1)		0.42855 (1)	$x = 0.218$ (this work)[c]
		0.41223 (2)		0.42858 (2)	$x = 0.225$ (this work)[c]
		0.41514 (8)		0.42556 (8)	$x = 0.267$ (this work)[c]
		0.41762 (3)		0.42152 (3)	$x_{max} = 0.321$ (this work)[c]
		0.8223		0.8565	supercell $a = 2a_0$, $c = 2c_0$ for Ce_2PdSi_3 [32]
		0.82622 (3)		1.71315 (5)	$x = 0.25$, supercell $a = 2a_0$, $c = 4c_0$; (this work)
τ_3, $Ce_2Pd_3Si_5$	*Ibam*,	0.9953	1.1810	0.5976	Annealed at 800 °C [24]
	$U_2Co_3Si_5$	0.9949	1.1816	0.5970	Annealed at 900 °C [50]
		0.9970	1.187	0.5990	Annealed at 900 °C [51]
		0.9951 (1)	1.1813 (2)	0.5973 (1)	(this work)
τ_4, $Ce_8Pd_{46}Si_{46}$	Unknown				(this work)
τ_5, Ce_3PdSi_3	*Immm*	0.41207 (1)	0.43026 (1)	1.84069 (4)	(this work)
	$Ba_3Al_2Ge_2$				
τ_6, $Ce(Pd_xSi_{1-x})_2$	*I*4$_1$/*amd*	0.4185		1.4602	$x = 0.38$ [26]
	$ThSi_2$	0.41842		1.4571	$x = 0.3$ [2]
					$0.338 \le x \le 0.387$ (this work)
		0.41837 (4)		1.4508 (2)	$x_{min} = 0.338$ (this work)
		0.41833 (1)		1.4563 (1)	$x = 0.360$ (this work)
		0.41818 (1)		1.4577 (1)	$x = 0.375$ (this work)
		0.41863 (1)		1.4599 (1)	$x_{max} = 0.387$ (this work)
τ_7, $CePd_{2-x}Si_{2+x}$	*I*4/*mmm*				$0 \le x \le 0.35$ [2]
<1510 [2]	$ThCr_2Si_2$	0.4212		0.998	$x = 0$ [52]
		0.4232		0.9911	$x = 0$ [25]
		0.42367		0.98880	$x = 0$, $T = 5$ K [53]
		0.42234		0.98962	$x = 0$, $T = 15$ K [53]
		0.4236		0.9874	$x = 0$ [54]
		0.4236		0.9900	$x = 0$ [55]
		0.42365		0.9899	$x = 0$ [2]

Table 1 (*continued*)

Phase	Space group	Lattice parameters (nm)			Comments
Temperature range (°C)	Prototype	*a*	*b*	*c*	
					$0 \le x \le 0.25$ (this work)
		0.42388 (4)		0.9878 (1)	$x_{min} = 0$ (this work)
		0.42159 (3)		0.9942 (1)	$x = 0.16$ (this work)
		0.42080 (4)		0.9995 (1)	$x_{max} = 0.25$ (this work)
τ_8, $Ce_3Pd_4Si_4$	*Immm*	0.41618 (1)	0.42640 (1)	2.45744 (7)	SC data (this work)
	$U_3Ni_4Si_4$	0.41768 (2)	0.42550 (2)	2.4475 (1)	(this work)
τ_9, CePdSi	$P2_1/c$	1.0810	0.5864	0.7891	SC data [26]
	PrPdSi		$\beta = 92.13°$		
		1.0813 (2)	0.58655 (3)	0.78923(5)	(this work)
			$\beta = 92.13$ (1)°		
τ_{10}, $Ce_4Pd_{29}Si_{14}$	$Fm\bar{3}m$	1.8010			SC data [27]
<1110 [2]	$Ce_4Pd_{29}Si_{14}$	1.8031 (2)			(this work)
τ_{11}, $CePd_2Si$	*Pnma*	0.7609	0.6877	0.5695	[28]
	YPd_2Si	0.7602 (1)	0.6874 (1)	0.5694 (1)	(this work)
τ_{12}, $Ce_{29}Pd_{49}Si_{22}$	Unknown				(this work)
τ_{13}, $Ce_{3-x}Pd_{20+x}Si_6$	$Fm\bar{3}m$				$0 \le x \le 1$ (this work)
<1240 [2]	$Co_{20}Al_3B_6$	1.2161			$x = 0$, SC data [29]
	at $x = 0$	1.2280			$x = 0$ [56]
		1.2272 (1)			$x = 0$ (this work)
	or $W_2Cr_{21}C_6$	1.2214 (1)			$x = 0.5$ (this work)
	at $x = 1$	1.2163 (1)			$x = 1$ (this work)
τ_{14}, Ce_3Pd_5Si	*Imma*	0.7377 (4)	1.3027 (4)	0.7580 (4)	SC data [30]
<950 [2]	*Ce_3Pd_5Si*	0.7438 (7)	1.311 (1)	0.767 (1)	[57]
					liquidus observed at 985 °C [2]
		0.73852 (5)	1.3039 (7)	0.76027 (5)	(this work)
τ_{15}, $Ce_{22}Pd_{67}Si_{11}$	Unknown				(this work)
τ_{16}, $Ce_2Pd_{14}Si$	*P4/nmm*	0.88832 (2)		0.69600 (2)	SC data (this work)
	$Ce_2Pd_{14}Si$				
$Ce_2Pd_{14-x}Si_{1+x}$					$0 \le x \le 0.32$ (this work)
		0.88789 (3)		0.69551 (2)	$x = 0.06$ (his work)
		0.88380 (7)		0.70394 (7)	$x_{max} = 0.32$ (this work)
τ_{17}, $Ce_5Pd_{77}Si_{18}$	Unknown				(this work)
τ_{18}, $CePd_{1-x}Si_x$	Unknown				$0.06 \le x \le 0.13$ (this work)
$CePdSi_2$[a]	Immm	0.4456	1.6495	0.8773	[31]
	$YIrGe_2$				
$Ce_2Pd_3Si_3$[b]	*Pmmn*	0.42040 (1)	0.42247 (1)	1.72444 (3)	(this work)
>800 °C	$Ce_2Rh_{1.35}Ge_{4.65}$				
$Ce_{\sim 12}Pd_{\sim 63}Si_{\sim 25}$[b]	Unknown				(this work)
>800 °C					
$Ce_{\sim 22}Pd_{\sim 61}Si_{\sim 17}$[b]	Unknown				(this work)
>800 °C					

[a] Phase not detected in the present work.
[b] Phase detected in as-cast alloy but does not participate in phase equilibria at 800 °C.
[c] Lattice parameters are given for AlB_2-subcell.

Ge as internal standard ($a_{Ge} = 0.5657906$ nm) using program STOE-WinXpow [3].

Single crystals (SC) were mechanically isolated from crushed alloys. Inspection on an AXS-GADDS texture goniometer assured high crystal quality, unit cell dimensions and Laue symmetry of the specimens prior to X-ray intensity data collection on a four-circle Nonius Kappa diffractometer equipped with a CCD area detector and employing graphite monochromated Mo$K\alpha$ radiation ($\lambda = 0.071073$ nm). Orientation matrix and unit cell parameters were derived using program DENZO [4]. No absorption corrections were necessary because of the rather regular crystal shape and small dimensions of the investigated specimens. The structures were solved by direct methods [5] and refined with the SHELXL-97 program [6]. Quantitative Rietveld refinement of the X-ray was performed with the FULLPROF program [7,8], employing internal tables for X-ray atomic form factors. Atom parameters were standardized with the aid of program STRUCTURE TIDY [9]. Structure and polyhedra were visualized using program DIAMOND [10].

All as-cast and annealed samples were polished via standard procedures and have been examined by scanning electron microscopy. Phase compositions were determined by Electron Probe Microanalysis (EPMA) on a Carl Zeiss LEO EVO 50XVP instrument with a Link EDX INCA Energy 450 system and a Carl Zeiss DSM 962 instrument equipped with a Link EDX system.

3. Binary systems

The Ce–Si binary phase diagram is based on a recent investigation by Bulanova et al. [11] amended by data on the existence of Ce_2Si_{3-x} ($x = 0.32$) [12]. The Pd–Si system was adopted from a recent review by Okamoto [13]. With respect to the rather slow decomposition kinetics of PdSi ($PdSi \Leftrightarrow Pd_2Si$+(Si) at 824 °C [14]) we have not included PdSi in our isothermal section at 800 °C, although PdSi is clearly observed in our ternary Ce–Pd–Si alloys after anneal at 800 °C up to 20 days (see Chapter 4.2). Furthermore, the compounds $Pd_{19}Si_{10}$ and $Pd_{39}Si_{20}$ with unknown structure, which were reported [15] to exist at the Si-rich side of Pd_2Si, could neither be detected in our EPMA (due to missing phase contrast) nor from XPD data (due to coincidence with the unknown structure of τ_4, $Ce_8Pd_{46}Si_{46}$).

As far as the binary system Ce–Pd as presented by Okamoto [16] is concerned, we observed discrepancies for (i) the stability

Table 2
Data on alloys from three-phase regions in the Ce–Pd–Si system at 800 °C.

Three-phase field	Phase	EPMA (at%)			Lattice parameters (nm)		
		Ce	Pd	Si	*a*	*b*	*c*
(Si)+$CeSi_2$+τ_1	(Si)	5.3	1.1	93.6	0.54292 (2)		
	$CeSi_2$	33.9	8.5	57.6	0.41979 (1)		1.4107 (1)
	τ_1	20.3	19.6	60.1	0.43205 (3)		0.9611 (1)
(Si)+τ_1+τ_3	(Si)	0.0	0.2	99.8	0.5426 (1)		
	τ_1	20.2	20.7	59.1	0.43191 (4)		0.9604 (1)
	τ_3	20.4	30.1	49.5	0.9949 (2)	1.1820 (2)	0.5978 (1)
(Si)+τ_3+τ_4	(Si)	0.0	0.6	99.4	0.5428 (2)		
	τ_3	19.5	30.4	50.1	0.9958 (2)	1.1822 (3)	0.5964 (1)
	τ_4	7.8	45.4	46.8		Unknown	
(Si)+Pd_2Si+τ_4	(Si)	0.0	0.0	100.0	0.54297 (5)		
	PdSi[a]	0.0	49.8	50.2	0.56116 (3)	0.33867 (2)	0.61476 (2)
	Pd_2Si	0.0	66.8	33.2	0.6531 (1)		0.34325 (5)
	τ_4	8.1	47.2	44.7		Unknown	
$CeSi_2$+τ_1+τ_3	$CeSi_2$	33.4	8.7	57.9	0.41961 (2)		1.4117 (1)
	τ_1	20.2	20.0	59.8	0.43199 (9)		0.9607 (2)
	τ_3	19.8	29.7	50.5	0.99514 (5)	1.1823 (1)	0.5976 (3)
CeSi+$CeSi_2$+τ_2	CeSi	49.5	0.0	50.5	0.8283 (1)	0.3967 (4)	0.59678 (9)
	$CeSi_2$	33.6	11.2	55.2	0.41860 (5)		1.4181 (3)
	τ_2[b]	33.7	14.3	52.0	0.41131 (2)		0.42820 (2)
$CeSi_2$+τ_2+τ_3	$CeSi_2$	32.9	12.5	54.6	0.41897 (1)		1.4202 (1)
	τ_2[b]	33.2	14.5	52.3	0.41174 (1)		0.42855 (1)
	τ_3	20.1	30.0	49.9	0.9949 (1)	1.1826 (1)	0.59758 (4)
CeSi+Ce_5Si_4+τ_5	CeSi	51.5	1.0	47.5	0.82880 (6)	0.39803 (4)	0.59593 (6)
	Ce_5Si_4	55.6	0.0	44.4	0.79520 (6)		1.5070 (3)
	τ_5	42.9	14.1	43.0	0.41197 (4)	0.43053 (4)	1.8415 (2)
CeSi+τ_2+τ_5	CeSi	49.5	0.00	50.5	0.8288 (1)	0.39723 (4)	0.59715 (8)
	τ_2[b]	33.5	17.8	48.7	0.41514 (8)		0.42556 (8)
	τ_5	43.1	13.4	43.5	–	–	–
τ_2+τ_5+τ_6	τ_2[b]	32.6	21.8	45.6	0.41725 (5)		0.42101 (5)
	τ_5	41.9	14.6	43.5	0.41138 (7)	0.42926 (7)	1.8448 (3)
	τ_6	33.1	22.9	44.0	0.41845 (5)		1.4526 (2)
τ_2+τ_6+τ_7	τ_2[b]	33.2	21.4	45.3	0.41762 (3)		0.42152 (3)
	τ_6	33.6	22.5	43.9	0.41837 (4)		1.4508 (2)
	τ_7	20.3	40.3	39.4	0.42403 (5)		0.9868 (2)
τ_2+τ_3+τ_7	τ_2[b]	33.2	14.8	52.0	0.41272 (1)		0.42853 (1)
	τ_3	20.1	29.9	50.0	0.99694 (3)	1.18244 (3)	0.59702 (1)
	τ_7	20.4	33.9	45.7	0.42117 (1)		0.99784 (3)
τ_3+τ_4+τ_7	τ_3	19.7	30.5	49.8	0.9959 (1)	1.1823 (1)	0.59768 (6)
	τ_4	7.2	46.6	46.2		Unknown	
	τ_7	19.8	35.2	45.0	0.42113 (3)		0.9980 (2)
Pd_2Si+τ_4+τ_7	Pd_2Si	0.0	65.4	34.6	0.65316 (5)		0.34327 (3)
	τ_4	7.9	45.4	46.7		Unknown	
	τ_7	20.1	34.8	45.1	0.42120 (4)		0.9988 (2)
Ce_5Si_4+τ_5+τ_{18}	Ce_5Si_4	55.4	5.3	39.3	0.79636 (6)		1.4979 (2)
	τ_5	42.8	14.8	42.4	0.41220 (2)	0.43042 (3)	1.8411 (2)
	τ_{18}	49.7	43.8	6.5		Unknown	
Ce_5Si_4+Ce_3Si_2+τ_{18}	Ce_5Si_4	56.0	7.1	36.9	0.79678 (6)		1.4937 (2)
	Ce_3Si_2	60.0	2.7	37.3	0.78021 (5)		0.43627 (3)
	τ_{18}	49.9	44.2	5.9		Unknown	
Ce_3Si_2+Ce_5Si_3+CePd	Ce_3Si_2	60.1	4.0	35.9	0.77992 (1)		0.43656 (1)
	Ce_5Si_3	62.7	4.1	33.2	0.78632 (5)		1.3816 (1)
	CePd	49.5	47.4	3.1	–	–	–
τ_5+τ_9+τ_{18}	τ_5	44.7	12.2	43.1	0.41198 (1)	0.42953 (1)	1.84524 (5)
	τ_9	33.8	32.7	33.5	1.08074 (4)	0.58626 (2) $\beta = 92.16\ (1)^\circ$	0.78830 (3)
	τ_{18}	50.4	46.1	3.5		Unknown	
τ_6+τ_8+τ_9	τ_6	33.5	25.8	40.7	0.41863 (1)		1.4599 (1)
	τ_8	27.3	36.2	36.5	0.41768 (2)	0.42550 (2)	2.4475 (1)
	τ_9	33.2	33.6	33.2	1.08103 (4)	0.58642 (2) $\beta = 92.14\ (1)^\circ$	0.78925 (3)
τ_6+τ_7+τ_8	τ_6	32.4	25.2	42.4	0.41849 (2)		1.4561 (2)
	τ_7	19.7	40.3	40.0	0.42398 (4)		0.9869 (1)
	τ_8	27.0	36.1	36.9	0.4180 (1)	0.4248 (1)	2.4445 (4)

Table 2 (*continued*)

Three-phase field	Phase	EPMA (at%)			Lattice parameters (nm)		
		Ce	Pd	Si	*a*	*b*	*c*
$\tau_8+\tau_9+\tau_{12}$	τ_8	27.4	37.0	35.6	0.41618 (5)	0.42615 (5)	2.4533 (4)
	τ_9	33.4	34.3	32.4	–	–	–
	τ_{12}	28.7	49.5	21.8		Unknown	
$\tau_8+\tau_{11}+\tau_{12}$	τ_8	27.1	37.1	35.8	0.41616 (5)	0.42632 (5)	2.4527 (3)
	τ_{11}	25.0	49.9	25.1	0.7607 (1)	0.6876 (1)	0.56969 (8)
	τ_{12}	28.7	48.9	22.4		Unknown	
$\tau_7+\tau_8+\tau_{11}$	τ_7	19.7	40.5	39.8	0.4240 (1)		0.9897 (3)
	τ_8	27.1	36.7	36.2	0.41635 (3)	0.42613 (3)	2.4517 (2)
	τ_{11}	24.7	50.3	25.0	0.7615 (1)	0.6873 (1)	0.5701 (1)
$\tau_7+\tau_{11}+\tau_{15}$	τ_7	19.6	40.6	39.8	0.42374 (2)		0.98694 (8)
	τ_{11}	24.8	50.1	25.1	–	–	–
	τ_{15}	22.7	65.6	11.7		Unknown	
$\tau_7+\tau_{13}+\tau_{15}$	τ_7	19.7	40.9	39.4	0.42429 (3)		0.9878 (1)
	τ_{13}	10.9	68.3	20.8	1.22783 (3)		
	τ_{15}	22.6	65.5	11.9		Unknown	
$\tau_7+\tau_{10}+\tau_{13}$	τ_7	19.6	40.2	40.2	0.42453 (3)		0.98647 (7)
	τ_{10}	8.5	61.4	30.1	1.80342 (7)		
	τ_{13}	10.6	68.2	21.2	1.22751 (4)		
$Pd_2Si+\tau_7+\tau_{10}$	Pd_2Si	0.0	48.1	47.9	0.64997 (7)		0.34286 (7)
	τ_7	19.7	40.3	40.0	0.42435 (3)		0.9875 (1)
	τ_{10}	8.5	62.0	29.5	1.80457 (7)		
$Ce_3Pd_4+CePd+\tau_9$	Ce_3Pd_4	43.5	56.0	0.5	1.3692 (2)		0.58230 (5)
	CePd	50.4	49.0	0.6	0.38893 (2)	1.0932 (1)	0.46229 (5)
	τ_9	34.5	33.4	31.9	1.0816 (1)	0.58655 (7)	0.78869 (9)
						$\beta = 92.11\ (1)^\circ$	
$Ce_3Pd_4+\tau_9+\tau_{14}$	Ce_3Pd_4	43.2	56.8	0.0	1.3699 (2)		0.5813 (1)
	τ_9	33.6	34.4	32.0	1.08163 (4)	0.58668 (2)	0.78929 (3)
						$\beta = 92.08\ (1)^\circ$	
	τ_{14}	33.5	55.0	11.5	0.7372 (1)	1.3052 (3)	0.7575 (1)
$Ce_3Pd_4+Ce_3Pd_5+\tau_{14}$	Ce_3Pd_4	43.3	56.7	0.0	1.3687 (3)		0.5821 (1)
	Ce_3Pd_5	37.6	62.4	0.0		Unknown	
	τ_{14}	34.1	54.6	11.3	0.73842 (4)	1.30423 (5)	0.76015 (4)
$Ce_3Pd_5+CePd_3+\tau_{14}$	Ce_3Pd_5	37.2	62.8	0.0		Unknown	
	$CePd_3$	24.3	69.6	6.1	0.42411 (4)		
	τ_{14}	33.5	55.6	10.9	0.7388 (1)	1.3031 (2)	0.7597 (1)
$CePd_3+\tau_{14}+\tau_{15}$	$CePd_3$	24.4	69.7	5.9	0.42431 (3)		
	τ_{14}	33.4	55.3	11.3	0.73851 (6)	1.3043 (1)	0.75976 (7)
	τ_{15}	22.7	66.1	11.2		Unknown	
$\tau_9+\tau_{12}+\tau_{14}$	τ_9	33.6	34.4	32.0	1.0820 (1)	0.58684 (4)	0.78931 (7)
						$\beta = 92.11\ (1)^\circ$	
	τ_{12}	28.9	48.9	22.2		Unknown	
	τ_{14}	33.2	55.7	11.1	0.7377 (2)	1.3042(3)	0.7604 (2)
$\tau_{12}+\tau_{14}+\tau_{15}$	τ_{12}	28.7	49.5	21.8		Unknown	
	τ_{14}	33.1	55.6	11.3	–	–	–
	τ_{15}	22.6	66.1	11.3		Unknown	
$\tau_{11}+\tau_{12}+\tau_{15}$	τ_{11}	24.5	49.8	25.7	0.76031 (9)	0.68741 (7)	0.56933 (8)
	τ_{12}	28.5	49.0	22.5		Unknown	
	τ	21.9	66.2	11.9		Unknown	
$CePd_3+\tau_{13}+\tau_{15}$	$CePd_3$	~25	~69	~6	0.42416 (2)		
	τ_{13}	10.9	68.7	20.4	1.22732 (7)		
	τ_5	22.3	66.8	10.9		Unknown	
$Pd_2Si+\tau_{10}+\tau_{13}$	Pd_2Si	0.0	66.7	33.3	0.64961 (2)		0.34338 (1)
	τ_{10}	9.0	62.0	29.0	1.80394 (5)		
	τ_{13}	10.5	68.8	20.7	1.22789 (3)		
$Pd_2Si+Pd_3Si+\tau_{13}$	Pd_2Si	0.0	67.6	32.4	0.6502 (1)		0.34317 (6)
	Pd_3Si	0.0	75.8	24.2	0.5747 (1)	0.7565 (1)	0.5253 (1)
	τ_{13}	6.7	73.4	19.9	1.21672 (8)		
$Pd_3Si+\tau_{13}+\tau_{17}$	Pd_3Si	0.0	75.0	25.0	0.5737 (8)	0.7556 (2)	0.5263 (1)
	τ_{13}	6.9	72.9	20.2	1.2150 (1)		
	τ_{17}	4.8	76.4	18.8		Unknown	
$CePd_3+\tau_{13}+\tau_{16}$	$CePd_3$	24.2	75.8	0.0	0.41439 (3)		
	τ_{13}	7.0	72.4	20.6	1.2151 (1)		
	τ_{16}	11.5	80.7	7.8	0.88380 (7)		0.70394 (7)

Table 2 (*continued*)

Three-phase field	Phase	EPMA (at%)			Lattice parameters (nm)		
		Ce	Pd	Si	*a*	*b*	*c*
$\tau_{13}+\tau_{16}+\tau_{17}$	τ_{13}	7.3	73.0	19.7	1.21462 (6)		
	τ_{16}	11.9	82.1	6.0	0.88743 (3)		0.69676 (4)
	τ_{17}	4.9	77.2	17.9		Unknown	
$CePd_7+\tau_{16}+L$	$CePd_7$	9.8	90.2	0.0	0.79458 (7)		
	τ_{16}	11.6	85.5	5.9	0.8880 (3)		0.6965 (1)
	L[c]	2.2	83.6	14.2			
$CePd_5+CePd_7+\tau_{16}$	$CePd_5$	16.4	81.5	2.1	–	–	–
	$CePd_7$	12.6	87.4	0.0	0.79519 (3)		
	τ_{16}	12.2	81.6	6.2	0.88789 (3)		0.69551 (2)
$CePd_3+CePd_5+\tau_{16}$	$CePd_3$	24.6	75.4	0.0	0.41307 (1)	–	–
	$CePd_5$	15.8	79.7	4.5	0.4021 (4)		
	τ_{16}	–	–	–	0.88531 (6)		0.70058 (6)

[a] Non-equilibrium phase.
[b] Lattice parameters are given for AlB_2-subcell.
[c] Eutectic composition.

range of $CePd_7$ and (ii) the crystal structure of Ce_3Pd_5. Our investigations are consistent with data of Bretschneider and Schaller [17] on the existence of $CePd_7$ at 800 °C in the composition range from 10.2 to 12.8 at% Ce. Secondly, our X-ray patterns recorded from Ce_3Pd_5 in as-cast state and after anneal at 800 °C are incompatible with the Th_3Pd_5-type structure reported by Kappler et al. [18], however, are in line with Thomson [19] who noted that Ce_3Pd_5 does not resemble the Th_3Pd_5 structure. The alloy $CePd_5$ annealed at 800 °C was found to contain both the hexagonal hT phase and the *fcc* lT phase, for which Kuwano et al. [20] with the aid of electron diffraction and high-resolution microscopy clearly revealed a superstructure that can not be recognized by simple X-ray powder diffraction. As reported in literature [21], we also were not able to quench the high-temperature modification β-CePd. However, refinement of X-ray single-crystal data, collected on a single crystal, which was isolated from the as-cast alloy $Ce_{60}Pd_{38}Si_2$, reveals an atomic arrangement isotypic with the structure type of FeB. Direct methods converged to $R_{F^2} = 0.032$ at residual electron densities smaller than $\pm 4.2\,e^-/Å^3$ resulting in a formula $Ce(Pd_{1-x}Si_x)$ $x = 0.07(1)$.

Crystallographic data pertinent to the Ce–Pd–Si system are summarized in Table 1. X-ray powder diffraction intensities for binary and unary phases reported in literature agree well with those observed in ternary Ce–Pd–Si alloys (Table 2).

4. Results and discussion

4.1. Crystal structure of ternary phases

Crystal structures for all those ternary compounds, which were already reported earlier (τ_1—$CePdSi_3$ ($BaNiSn_3$-type) [2,22], τ_3—$Ce_2Pd_3Si_5$ ($U_2Co_3Si_5$-type) [23], τ_6—$Ce(Pd_xSi_{1-x})_2$ ($ThSi_2$-type) [24], τ_7—$CePd_{2-x}Si_{2+x}$ ($ThCr_2Si_2$-type) [25], τ_9—CePdSi (PrPdSi-type) [26], τ_{10}—$Ce_4Pd_{29}Si_{14}$ (own type) [27], τ_{11}—$CePd_2Si$ (YPd_2Si-type, ordered version of Fe_3C-type) [28], τ_{13}—$Ce_{3-x}Pd_{20+x}Si_6$ ($Co_{20}Al_3B_6$-type) [29], τ_{14}—Ce_3Pd_5Si (own type) [30]), were found to be consistent with data in literature. $CePdSi_2$ ($YIrGe_2$-type) reported to be stable at 1000 °C [31] does not participate in the equilibria at 800 °C.

$Ce(Pd_xSi_{1-x})_2$ with AlB_2-type [22,24] is observed only in the as-cast state whereas the alloys annealed at 800 °C reveal a set of additional reflections indicating superstructure formation. All X-ray reflections were indexed on a hexagonal cell with lattice parameters $a = 0.82638(6)$ nm and $c = 1.7134(1)$ nm indicating an $a = 2a_0$ and $c = 4c_0$ supercell of the AlB_2-type. These data are in line with observations of a superstructure $a = 2a_0$ and $c = 2c_0$ for composition Ce_2PdSi_3 [32]. Our attempts to select a single crystal suitable for structure determination was unsuccessful and therefore τ_2—$Ce(Pd_xSi_{1-x})_2$ is denoted in the manuscript as AlB_2-derivative.

For a series of new compounds, crystal structures were derived either from single crystals or by Rietveld analyses. Crystal data and extension of solid solutions are summarized in Tables 1, 3 and 4. Structural chemistry of the new compounds τ_5—Ce_3PdSi_3 ($Ba_3Al_2Ge_2$-type), τ_8—$Ce_3Pd_4Si_4$ ($U_3Ni_4Si_4$-type), τ_{13}—$Ce_2Pd_{21}Si_6$ ($W_2Cr_{21}C_6$-type) and solution phases follow the characteristics already outlined for the prototype structures, while the new ternary compound τ_{16}—$Ce_2Pd_{14}Si$ crystallizes with a unique tetragonal structure.

Five ternary phases τ_4—$Ce_{\sim 8}Pd_{\sim 46}Si_{\sim 46}$, τ_{12}—$Ce_{\sim 29}Pd_{\sim 49}Si_{\sim 22}$, τ_{15}—$Ce_{\sim 22}Pd_{\sim 67}Si_{\sim 11}$, τ_{17}—$Ce_{\sim 5}Pd_{\sim 77}Si_{\sim 18}$ and τ_{18}—$CePd_{1-x}Si_x$ with unknown structures were detected. Besides the ternary phases, which are stable at 800 °C (Table 1), a new high-temperature compound $Ce_2Pd_3Si_3$ was observed in as-cast conditions and after anneal at 1100 °C. $Ce_2Pd_3Si_3$, however, is unstable at 800 °C. Rietveld refinement for $Ce_2Pd_3Si_3$ yields isotypism with the structure type of $Ce_2Rh_{1.35}Ge_{4.65}$ [33] (*Pmmn*, $Z = 2$, $a = 0.42040(1)$, $b = 0.42247(1)$, $c = 1.72444(3)$ nm; see Table 4).

Two further compounds with structures still unknown and compositions $Ce_{\sim 12}Pd_{\sim 63}Si_{\sim 25}$ and $Ce_{\sim 22}Pd_{\sim 61}Si_{\sim 17}$ (in at% from EPMA) were detected in as-cast state, however, these phases decompose after anneal at 800 °C (Fig. 1).

Compositional dependences of unit cell parameters as a function of Si/Pd exchange for τ_2—$Ce(Pd_xSi_{1-x})_2$ (AlB_2-derivative type, $0.215 \le x \le 0.321$), τ_6—$Ce(Pd_xSi_{1-x})_2$ ($ThSi_2$-type, $0 \le x \le 0.188$ and $0.338 \le x \le 0.387$) and τ_7—$CePd_{2-x}Si_{2+x}$ ($ThCr_2Si_2$-type, $0 \le x \le 0.25$) are shown in Fig. 2. One can see that within homogeneity regions of both phases with $ThSi_2$-type structure the *c*-lattice parameter increases significantly while the *a*-parameter is almost unaffected by Pd/Si substitution. A different trend is observed for τ_2—$Ce(Pd_xSi_{1-x})_2$ (AlB_2-derivative type) and τ_7—$CePd_{2-x}Si_{2-x}$ ($ThCr_2Si_2$-type): the *a*-lattice parameter increases while the *c*-lattice parameter decreases with increase of Pd content. Note that the resulting atomic volume for these phases increases with Pd content in line with the difference of the atomic radii of the elements.

Table 3
X-ray single-crystal data for τ_{18}—$CePd_{1-x}Si_x$, τ_8—$Ce_3Pd_4Si_4$ and τ_{16}—$Ce_2Pd_{14}Si$ (Mo$K\alpha$ radiation, room temperature); structure data standardized with program *Structure Tidy* [9].

Parameter/compound	**τ_{18}–$CePd_{1-x}Si_x$**	**τ_8—$Ce_3Pd_4Si_4$**	**τ_{16}—$Ce_2Pd_{14}Si$**
Alloy composition (at%)	$Ce_{60}Pd_{38}Si_2$	$Ce_{27.3}Pd_{36.3}Si_{36.4}$	$Ce_{11.7}Pd_{82.4}Si_{5.9}$
Crystal size (μm)	$30\times30\times30$	$50\times50\times50$	$30\times30\times30$
Space group	*Pnma* (no. 62)	*Immm* (no. 71)	*P4/nmm* (no. 129)
Prototype	FeB	$U_3Ni_4Si_4$	$Ce_2Pd_{14}Si$
Pearson symbol	*oP*8	*oI*22	*tP*34
Lattice parameters (nm)	$a=0.74422$ (5) $b=0.45548$ (3) $c=0.58569$ (4)	$a=0.41618$ (1) $b=0.42640$ (1) $c=2.45744$ (7)	$a=0.88832$ (2) $c=0.69600$ (2)
Volume (nm^3)	0.19854 (2)	0.4361 (3)	0.54922 (2)
μ_{abs} (mm^{-1})	29.11	23.84	30.42
2θ range up to (°)	72.62	72.57	72.23
Reflections in refinement	$390\geq4\sigma(F_o)$ of 518	$602\geq4\sigma(F_o)$ of 640	$676\geq4\sigma(F_0)$ of 768
Index range	$-12\leq h\leq12$ $-7\leq k\leq7$ $-9\leq l\leq9$	$-6\leq h\leq6$ $-7\leq k\leq7$ $-38\leq l\leq39$	$-14\leq h\leq14$ $-14\leq k\leq14$ $-11\leq l\leq11$
Calculated density (g/cm^3)	7.59	7.30	10.87
Number of variables	15	25	32
$R_F^2=\sum\lvert F_o^2-F_c^2\rvert/\sum F_0^2$	0.032	0.022	0.025
R_{Int}	0.020	0.012	0.047
wR_2	0.071	0.060	0.038
GOF	1.053	1.192	1.139
Extinction	0.0023 (7)	0.0039 (2)	0.00020 (5)
Atom parameters			
Atom site 1	**4 Ce1** in 4*c* (*x*,1/4,*z*); $x=0.18057$ (6) $z=0.63849$ (8)	**2 Ce1** in 2*a* (0,0,0)	**2 Ce1** in 2*c* (1/4,1/4,*z*); $z=0.06217$ (9)
occ.	1.00 (−)	1.00 (−)	1.00 (−)
U_{11},U_{22},U_{33} (in $10^2\,nm^2$)	0.0159 (2), 0.0235 (3),0.0176 (3)	0.0076 (2), 0.0085 (2), 0.0087 (2)	0.0087 (2), 0.0087 (2),0.0082 (3)
U_{23},U_{13},U_{12} (in $10^2\,nm^2$)	0, 0.0001 (2), 0	0, 0, 0	0, 0, 0
Atom site 2	**4 M1** in 4*c* (*x*, 1/4,*z*); $x=0.04150$ (11), $z=0.14235$ (14)	**4 Ce2** in 4*j* (1/2,0,*z*); $z=0.35283$ (1)	**2 Ce2** in 2*b* (3/4,1/4,1/2)
occ.	0.93 (1) Pd+0.07 Si	1.00(−)	1.00(−)
U_{11},U_{22},U_{33} (in $10^2\,nm^2$)	0.0285(4), 0.0176(3), 0.0288(5)	0.0077 (2), 0.0075 (2), 0.0068 (1)	0.0118 (2), 0.0118 (2), 0.0079 (3)
U_{23},U_{13},U_{12} (in $10^2\,nm^2$)	0, −0.0033 (3), 0	0, 0, 0	0, 0, 0
Atom site 3		**4 Pd1** in 4*j* (1/2,0,); $z=0.09827$ (2)	**8 Pd1** in 8*j* (*x*,*x*,*z*); $x=0.08360$ (3), $z=0.38531$(6)
occ.		1.00 (−)	1.00 (−)
U_{11},U_{22},U_{33} (in $10^2\,nm^2$)		0.0129 (2), 0.0073 (2), 0.0081 (2)	0.0099 (1), 0.0099 (1), 0.0093 (2)
U_{23},U_{13},U_{12} (in $10^2\,nm^2$)		0, 0, 0	0.0000 (1), 0.0000 (1), −0.0008 (1)
Atom site 4		**4 Pd2** in 4*i* (0,0,*z*); $z=0.24917$ (2)	**8 Pd2** in 8*i* (1/4,*y*,*z*); $y=0.01805$ (5), $z=0.73901$ (6)
occ.		1.00 (−)	1.00 (−)
U_{11},U_{22},U_{33} (in $10^2\,nm^2$)		0.0086 (2), 0.0090 (2), 0.0076 (2)	0.0112 (2), 0.0080 (2), 0.0102 (2)
U_{23},U_{13},U_{12} (in $10^2\,nm^2$)		0, 0, 0	0.0014 (1), 0, 0
Atom site 5		**4 Si1** in 4*j* (1/2,0,*z*); $z=0.19737$ (6)	**8 Pd3** in 8*i* (1/4,*y*,*z*); $y=0.59995$ (5), $z=0.14875$ (6)
occ.		1.00 (−)	1.00 (−)
U_{11},U_{22},U_{33} (in $10^2\,nm^2$)		0.0082 (6), 0.0081 (6), 0.0081 (6)	0.0077 (2), 0.0090 (2), 0.0114 (2)
U_{23},U_{13},U_{12} (in $10^2\,nm^2$)		0, 0, 0	0.0012 (1), 0, 0
Atom site 6		**4 Si2** in 4*i* (0,0,*z*); $z=0.45212$(6)	**4 Pd4** in 4*d* (0,0,0)
occ.		1.00 (−)	1.00 (−)
U_{11},U_{22},U_{33} (in $10^2\,nm^2$)		0.0089 (6), 0.0017 (5), 0.0055 (5)	0.0094 (2), 0.0094 (2), 0.0106 (2)
U_{23},U_{13},U_{12} (in $10^2\,nm^2$)		0, 0, 0	−0.0002 (1), −0.0002 (1), 0.0024 (2)
Atom site 7			**2 Si1** in 2*c* (1/4,1/4,*z*); $z=0.5498$ (5)
occ.			1.00 (−)
U_{11},U_{22},U_{33} (in $10^2\,nm^2$)			0.009 (1), 0.009 (1), 0.009 (1)
U_{23},U_{13},U_{12} (in $10^2\,nm^2$)			0, 0, 0
Residual density ($e/Å^3$); max; min	4.2; −2.4	1.8; −2.1	1.8; −2.2
Principal mean square atomic displacements of U_{ij}	Ce1 0.0235 0.0176 0.0159 Pd1 0.0319 0.0254 0.0176	Ce1 0.0087 0.0085 0.0075 Ce2 0.0077 0.0075 0.0068 Pd1 0.0129 0.0081 0.0073 Pd2 0.0090 0.0086 0.0076 Si1 0.0082 0.0081 0.0081	Ce1 0.0087 0.0087 0.0082 Ce2 0.0119 0.0119 0.079 Pd3 0.0107 0.0093 0.0091 Pd4 0.0112 0.0109 0.0073 Pd5 0.0119 0.0085 0.0077

Table 4
Crystallographic data for τ_5—Ce_3PdSi_3, τ_{13}—$Ce_2Pd_{21}Si_6$ and $Ce_2Pd_3Si_3$ (X-ray powder diffraction at room temperature, image plate, Cu$K\alpha$1 radiation); standardized with program *Structure Tidy* [9].

Parameter/compound	**τ_5—Ce_3PdSi_3**	**τ_{13}—$Ce_2Pd_{21}Si_6$**	**$Ce_2Pd_3Si_3$**[a]
Composition, EPMA (at%)	$Ce_{42.4}Pd_{14.5}Si_{43.1}$	$Ce_{6.9}Pd_{72.8}Si_{20.3}$	$Ce_{24.6}Pd_{36.7}Si_{38.7}$
Composition from refinement (at%)	$Ce_{42.9}Pd_{13.7}Si_{43.4}$	$Ce_{6.9}Pd_{72.4}Si_{20.7}$	$Ce_{25}Pd_{37.5}Si_{37.5}$
Formula from refinement	$Ce_3Pd_{0.96}Si_{3.04}$	$Ce_2Pd_{21}Si_6$	$Ce_2Pd_3Si_3$
Space group	*Immm* (no. 71)	*Fm*$\bar{3}$*m* (no. 225)	*Pmmn* (no. 59)
Pearson symbol	*oI*14	*cF*116	*oP*16
Prototype	$Ba_3Al_2Ge_2$	$W_2Cr_{21}C_6$	$Ce_2Rh_{1.35}Ge_{4.65}$
Lattice parameters, (nm)	$a = 0.41207$ (1)	$a = 1.21527$ (2)	$a = 0.42040$ (1)
(Ge standard)	$b = 0.43026$ (1)		$b = 0.42247$ (1)
	$c = 1.84069$ (4)		$c = 1.72444$ (3)
Reflections measured	111	74	195
2θ range, (deg)	$8 \le 2\theta \le 90$	$8 \le 2\theta \le 90$	$8 \le 2\theta \le 90$
Number of variables	26	21	32
$R_F = \sum\|F_o - F_c\| / \sum F_o$	0.050	0.037	0.040
$R_I = \sum\|I_o - I_c\| / \sum I_o$	0.054	0.033	0.044
$R_{wP} = [\sum w_i\|y_{oi} - y_{ci}\|^2 / \sum w_i\|y_{oi}\|^2]^{1/2}$	0.035	0.030	0.021
$R_P = \sum\|y_{oi} - y_{ci}\| / \sum\|y_{oi}\|$	0.026	0.021	0.014
$R_e = [(N-P+C) / \sum w_i y_{oi}^2]^{1/2}$	0.023	0.014	0.013
$\chi^2 = (R_{wP}/R_e)^2$	2.4	4.7	2.2
Atom parameters			
Atom site 1	**4 Ce1** in 4*j* (1/2, 0, *z*);	**8 Ce1** in 8*c* (1/4,1/4,1/4)	**2 Ce1** in 2*b* (1/4,3/4,*z*);
	$z = 0.18512$ (4)		$z = 0.8525$ (2)
occ.	1.00 (−)	1.00 (−)	1.00 (−)
B_{iso} (10^2 nm^2)	0.40 (1)	0.75 (2)	0.72 (1)
Atom site 2	**2 Ce2** in 2*a* (0, 0, 0)	**4 Pd1** in 4*a* (0,0,0)	**2 Ce2** in 2*a* (1/4,1/4,*z*);
			$z = 0.6442$ (2)
occ.	1.00 (−)	1.00 (−)	1.00 (−)
B_{iso} (10^2 nm^2)	0.72 (1)	0.61 (3)	1.03 (2)
Atom site 3	**4 Si1** in 4*j* (1/2, 0, *z*);	**32 Pd2** in 32*f* (*x*,*x*,*x*);	**2 Pd1** in 2*b* (1/4,3/4,*z*);
	$z = 0.3626$ (2)	$x = 0.38573$ (2)	$z = 0.5011$ (3)
occ.	1.00 (−)	1.00 (−)	1.00 (−)
B_{iso} (10^2 nm^2)	0.46 (1)	0.84 (1)	0.42 (1)
Atom site 4	**4 M** in 4*j* (1/2, 0, *z*);	**48 Pd3** in 48*h* (0,*y*,*y*);	**2 Pd2** in 2*a* (1/4,1/4,*z*);
	$z = 0.43637$ (9)	$y = 0.17222$ (2)	$z = 0.0023$ (3)
occ.	0.52 (1) Si+0.48 Pd	1.00 (−)	1.00 (−)
B_{iso} (10^2 nm^2)	0.39 (1)	0.96 (1)	0.55 (1)
Atom site 5		**24 Si1** in 24*e* (*x*,0,0);	**2 Si1** in 2*b* (1/4,3/4,*z*);
		$x = 0.2668$ (2)	$z = 0.0698$ (4)
occ.		1.00 (−)	1.00 (−)
B_{iso} (10^2 nm^2)		0.47 (4)	0.71 (4)
Atom site 6			**2 Si2** in 2*a* (1/4,1/4,*z*);
			$z = 0.4103$ (7)
occ.			1.00 (−)
B_{iso} (10^2 nm^2)			0.71 (4)
Atom site 7			**2 M1** in 2*b* (1/4,3/4,*z*);
			$z = 0.2151$ (3)
occ.			0.46 (2) Pd+0.54 Si[b]
B_{iso} (10^2 nm^2)			0.71 (4)
Atom site 8			**2 M2** in 2*a* (1/4,1/4,*z*);
			$z = 0.2877$ (5)
Occ.			0.54 (2) Pd+0.46 Si[b]
B_{iso} (10^2 nm^2)			0.71 (4)

[a] In alloy quenched from 1100 °C. Compound does not participate in equilibria at 800 °C.
[b] Pd/Si ratio was fixed after EPMA.

4.1.1. Rietveld refinement of τ_5—Ce_3PdSi_3 with $Ba_3Al_2Ge_2$-type

The ternary compound Ce_3PdSi_3, detected in an alloy with nominal composition $Ce_{43}Pd_{14}Si_{43}$, forms incongruently and consequently the as-cast alloy contains significant amounts of secondary phases: τ_2—$Ce(Pd_xSi_{1-x})_2$, CeSi and $Ce_5(Si_{1-x}Pd_x)_4$. Rietveld refinement for Ce_3PdSi_3 yields isotypism with the structure type of $Ba_3Al_2Ge_2$ (*Immm*, Z = 2, $a = 0.41207(1)$, $b = 0.43026(1)$, $c = 1.84069(4)$ nm; see Table 4). Palladium and silicon atoms randomly share only the 4*j* site in a ratio 0.48(1): 0.52(1). Despite statistical distribution of palladium and silicon atoms the compound has a limited homogeneity region at 800 °C that is smaller than 1 at%. A refinement for a crystallographic model with splitting of this site into two 2*a* sites (0,0,*z*) in the lower symmetric space group *Imm*2 does not support full atom order of the structure ($R_F = 0.05$).

4.1.2. The crystal structure of τ_8—$Ce_3Pd_4Si_4$ with $U_3Ni_4Si_4$-type

A single crystal, broken from as-cast alloy with composition $Ce_{28}Pd_{42}Si_{30}$ (nominal composition in at%) revealed orthorhombic symmetry with space group *Immm* and lattice parameters: $a = 0.41618(1)$, $b = 0.42640(1)$, $c = 2.45744(7)$ nm. Direct methods yielded a completely ordered atom arrangement isotypic with the structure type of $U_3Ni_4Si_4$, which is characterized by a stacking of $BaAl_4$- and AlB_2-type layers. Results of the refinement for $Ce_3Pd_4Si_4$, which converged to $R_{F^2} = 0.022$ with residual

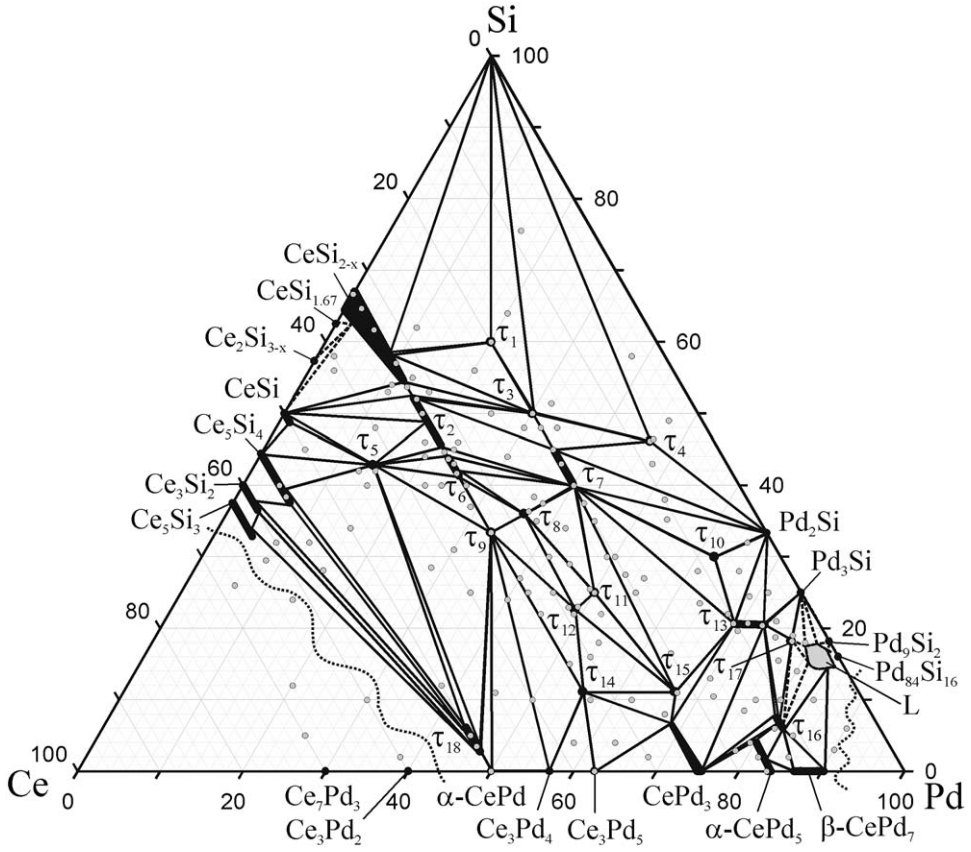

Fig. 1. Isothermal sections of the ternary system Ce–Pd–Si at 800 °C. Light gray circles indicate the samples in the investigation.

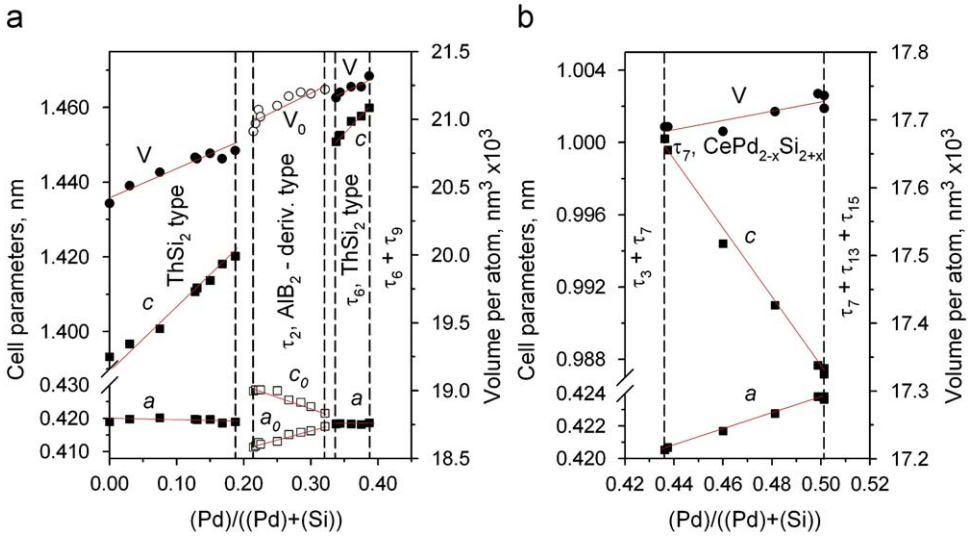

Fig. 2. Compositional dependences of cell parameters and average volume per atom for $Ce(Pd_xSi_{1-x})_2$ (a) and τ_7—$CePd_{2-x}Si_{2+x}$ (b).

electron densities smaller than $\pm 2.1\,e^-/Å^3$, are summarized in Table 3.

4.1.3. Rietveld refinement of τ_{13}—$Ce_{3-x}Pd_{20+x}Si_6$

EPMA of ternary alloys containing τ_{13} shows a homogeneity range from 6.9 to 10.3 at% Ce at a constant Si content of 20.3(5) at%. This observation suggests Pd/Ce substitution in the crystal structure resulting in the formula $Ce_{3-x}Pd_{20+x}Si_6$ ($0 \le x \le 1$). Rietveld refinements (Table 4) performed for compositions $Ce_3Pd_{20}Si_6$ and $Ce_2Pd_{21}Si_6$ confirmed that the cerium position in 4*a* in $Ce_3Pd_{20}Si_6$ ($Co_{20}Al_3B_6$-type structure [9], $a = 1.2272(1)$ nm) is completely replaced by palladium in $Ce_2Pd_{21}Si_6$ ($W_2Cr_{21}C_6$-type structure, $a = 1.2163(1)$ nm). The alternative crystallographic model with vacancies in the 4*a* site was rejected due to a significant disagreement between compositions obtained from Rietveld refinement and EPMA.

Table 5
Interatomic distances (nm) in $Ce_2Pd_{14}Si$ ($|\Delta| < 0.0001$ nm).

CA	L	d	CA	L	d	CA	L	d	CA	L	d
Ce1	-4Pd2	0.3050	Pd1	-1Si1	0.2383	Pd2	-1Si1	0.2445	Pd3	-2Pd4	0.2606
CN16	-4Pd1	0.3070	CN14	-1Pd1	0.2638	CN14	-2Pd3	0.2838	CN12	-1Pd3	0.2666
	-4Pd3	0.3167		-2Pd3	0.2748		-2Pd4	0.2874		-2Pd1	0.2748
	-4Pd4	0.3170		-1Pd4	0.2880		-1Ce2	0.2905		-1Ce2	0.2784
				-2Pd2	0.2930		-2Pd2	0.2914		-2Pd3	0.2800
Ce2	-4Pd3	0.2784		-2Pd1	0.2956		-2Pd1	0.2930		-2Pd2	0.2838
CN16	-4Pd2	0.2905		-1Ce1	0.3070		-1Pd3	0.3038		-1Pd2	0.3038
	-8Pd1	0.3407		-2Pd2	0.3216		-1Ce1	0.3050		-1Ce1	0.3167
				-2Ce2	0.3407		-2Pd1	0.3216			
Si1	-4Pd1	0.2383							Pd4	-4Pd3	0.2606
CN8	-4Pd2	0.2445							CN12	-4Pd2	0.2874
										-2Pd1	0.2880
										-2Ce1	0.3170

CA—central atom, L—ligand, d—distance, CN—coordination number.

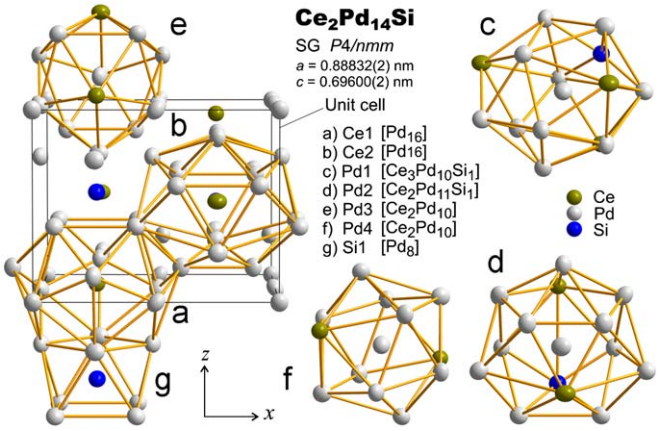

Fig. 3. Crystal structure of τ_{16}—$Ce_2Pd_{14}Si$ and coordination polyhedra of the atoms in a projection on the *xz* plane. Atoms are presented as displacement ellipsoids.

Both structure types $Ce_3Pd_{20}Si_6$ ($x = 0$) and $Ce_2Pd_{21}Si_6$ ($x = 1$) belong to a single-phase region $Ce_{3-x}Pd_{20+x}Si_6$ at 800 °C. Confirmation of this follows from the investigation of the alloy $Ce_{3-x}Pd_{20+x}Si_6$ ($x = 0.5$) which reveals a single-phase cubic structure with a lattice parameter a = 1.2214(1) nm right on the interpolation line of the two boundary compositions at $x = 0.1$. Furthermore, no split of the diffraction lines was observed in contrast to the existence of individual cubic phases $Ce_3Pd_{20}Si_6$ and $Ce_2Pd_{21}Si_6$ separated by a two-phase region.

4.1.4. *The crystal structure of τ_{16}—$Ce_2Pd_{14}Si$*

The X-ray diffraction pattern of a single crystal was indexed with tetragonal symmetry: space group *P4/nmm* and lattice parameters $a = 0.88832(2)$, $c = 0.69600(2)$ nm. Direct methods yielded a completely ordered atom arrangement with a new structure-type $Ce_2Pd_{14}Si$. Structure parameters and results of the refinement for $Ce_2Pd_{14}Si$, which converged to $R_{F^2} = 0.025$ with residual electron densities smaller than $\pm 2.2\ e^-/Å^3$, are summarized in Table 3. Interatomic distances in $Ce_2Pd_{14}Si$ are listed in Table 5. The composition derived from the refinement is in perfect agreement with EPMA.

The structure of $Ce_2Pd_{14}Si$ is shown in Fig. 3 in a projection on the *xz* plane. The structure can be presented as chains of Ce2–Si1–Ce2 (0.44551 nm) and Ce1–Pd3–Pd3–Ce1 (0.31665 and 0.26658 nm) atoms surrounded by infinite nets of Pd atoms (Fig. 3). Coordination polyhedra of all atoms are shown in Fig. 3. The coordination polyhedron around Si1 is a square antiprism (CN = 8), coordination polyhedra around Pd1 and Pd2 atoms include 14 atoms, and coordination figures around Pd3 and Pd4 atoms are distorted Franck–Kasper polyhedra (CN = 12). Cerium atoms are symmetrically surrounded by 16 Pd atoms forming slightly distorted Franck–Kasper polyhedra.

There is a short interatomic distance Ce2–Pd3 in the structure (Table 5). This bond length of 0.27845 nm is much smaller than the normal distance between cerium and palladium ($d_{Ce1-Pd2}$ 0.30503 nm). We suggest that the valence of Ce2 in $Ce_2Pd_{14}Si$ is higher than 3, whereas the ground state of Ce1 is expected to be trivalent.

4.2. *Phase relations; isothermal section Ce–Pd–Si at 800 °C*

Phase relations in the ternary system at 800 °C are shown in Fig. 1. Data on composition and lattice parameters for equilibrium phases that are involved in three-phase equilibria at 800 °C are listed in Table 2. Phase equilibria are characterized by the absence of cerium solubility in the various palladium silicides. However, mutual solubilities among cerium silicides and cerium–palladium compounds are significant. The random substitution of the almost equal-sized atom species palladium and silicon is reflected in extended homogeneous regions at constant Ce-content for several binary and ternary compounds such as for τ_2—$Ce(Pd_xSi_{1-x})_2$, τ_6—$Ce(Pd_xSi_{1-x})_2$ and τ_7—$CePd_{2-x}Si_{2+x}$.

The isothermal section at 800 °C for the composition range above 60 at% Ce involves equilibrium with a liquid phase and was not investigated in detail. A liquid phase region was also found at 800 °C near the Pd–Si binary. Microstructure of alloy $Ce_6Pd_{84}Si_{10}$ after anneal at 800 °C (Fig. 4a) clearly shows that the sample was in liquid–solid state: big grains of τ_{16} and $CePd_7$ were growing in equilibrium with a eutectic liquid of composition $Ce_{\sim 2}Pd_{\sim 84}Si_{\sim 14}$. The eutectic structure (see inset in Fig. 4a) reveals nicely shaped crystals of τ_{16} embedded in a eutectic containing Pd_9Si_2.

The compound τ_4—$Ce_{\sim 8}Pd_{\sim 46}Si_{\sim 46}$ with unknown structure likely forms from a peritectoid reaction. τ_4 was not observed in as-cast samples but was found in equilibrium with τ_3 and τ_7 at 800 °C. The microstructure of the as-cast sample $Ce_{15}Pd_{35}Si_{50}$ in Fig. 4c shows big primary grains of τ_7 followed by secondary crystallization of PdSi and (Si). The eutectic has the composition $Ce_{\sim 2}Pd_{\sim 54}Si_{\sim 43}$. After annealing at 800 °C, the structure of the sample drastically changes (Fig. 4d) via partial decomposition of τ_7 under formation of τ_4 and τ_3 in form of a laminar structure. Similarly, $Ce_{\sim 12}Pd_{\sim 63}Si_{\sim 25}$ (X_1, unknown structure) and $Ce_{\sim 22}Pd_{\sim 61}Si_{\sim 17}$ (X_2, unknown structure) were detected in as-cast

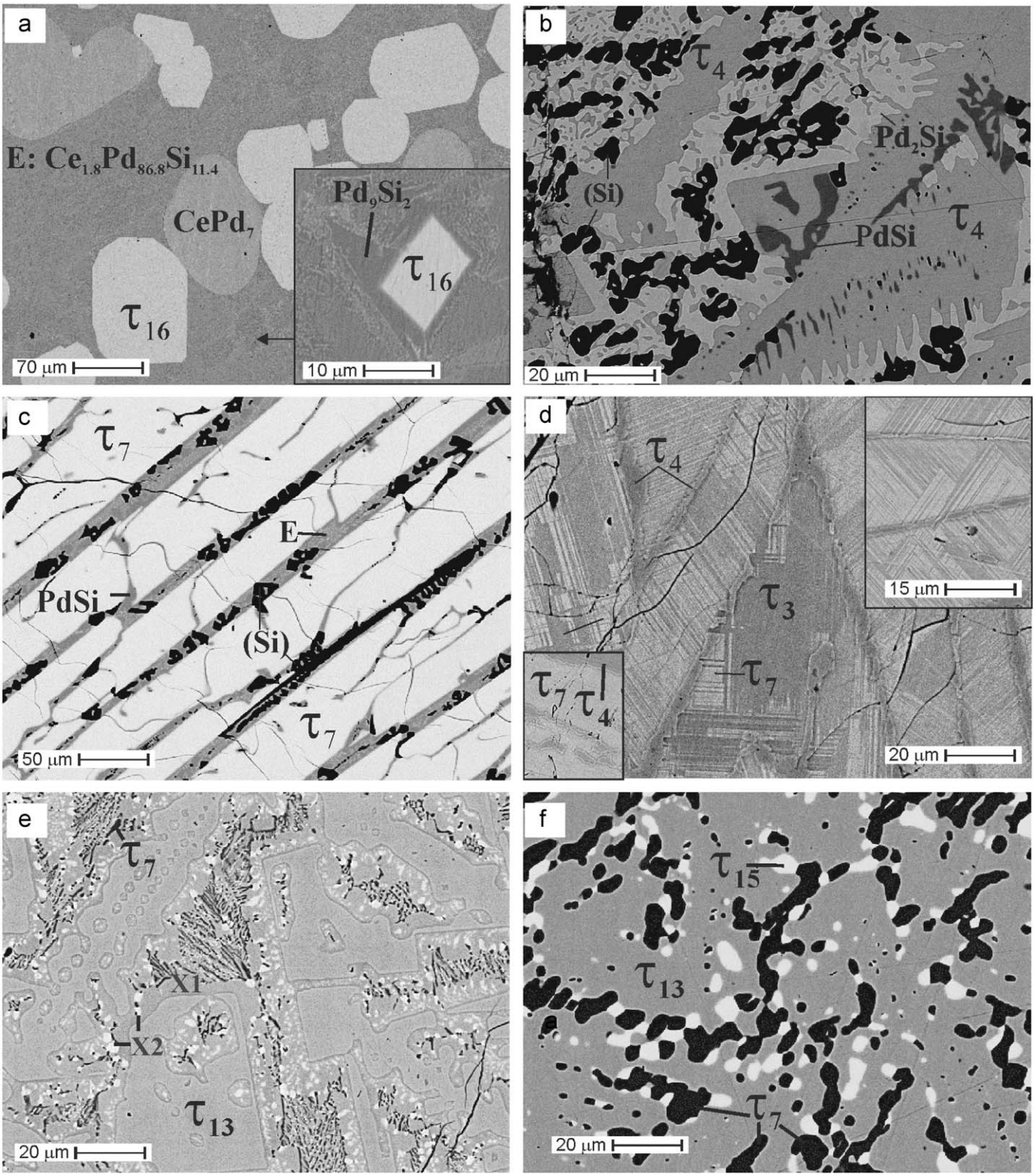

Fig. 4. Microstructure of selected Ce–Pd–Si alloys: $Ce_6Pd_{84}Si_{10}$ (*a*, 800 °C), $Ce_4Pd_{38}Si_{58}$ (*b*, 800 °C), $Ce_{15}Pd_{35}Si_{50}$ (*c*, as-cast; *d*, 800 °C), $Ce_{13}Pd_{63.5}Si_{23.5}$ (*e*, as-cast; *f*, 800 °C). $X_1 = Ce_{\sim 12}Pd_{\sim 63}Si_{\sim 25}$, $X_2 = Ce_{\sim 22}Pd_{\sim 61}Si_{\sim 17}$.

samples (Fig. 4e) but they do not participate in the equilibria at 800 °C. The same situation was met for $CePd_{1-x}Si_x$ ($x = 0.07$) for which the FeB-type structure was established in the present work in as-cast alloys. Annealing at 800 °C, however, reveals an X-ray diffraction pattern that could not be attributed to any binary or ternary Ce–Pd–Si phase (Table 1). EPMA for this new ternary compound τ_{18} reveals an approximate formula $CePd_{1-x}Si_x$ within a small homogeneity region $0.06 \leq x \leq 0.13$.

Physical properties of some of the ternary compounds are part of forthcoming publications.

Acknowledgments

This research was supported by the Austrian National Science Foundation FWF project P18054-Phy. The authors are grateful to the Russian Foundation of Basic Research, project no. 08-03-01072_a, and to the bilateral WTZ Austria–Russia, project 17/06.

Appendix A. Supporting Information

Supplementary data associated with this article can be found in the online version at doi:10.1016/j.jssc.2009.06.022.

References

[1] A. Gribanov, P. Rogl, J.D. Seropegin, in: W. Martienssen (Ed.), Landolt–Börnstein—Group IV Physical Chemistry, vol. 11B, Springer, Berlin, 2006, p. 340.
[2] Y.D. Seropegin, A.V. Gribanov, O.L. Kubarev, A.I. Tursina, O.I. Bodak, J. Alloys Compd. 317–318 (2001) 320.
[3] STOE WINXPOW (Version 1.06), Stoe & Cie GmbH, Darmstadt, Germany, 1999.
[4] Nonius, Kappa CCD Program Package: COLLECT, DENZO, SCALEPACK, SORTAV, Nonius BV, Delft, The Netherlands, 1998.
[5] G.M. Sheldrick, Acta Crystallogr. A 46 (1990) 467.
[6] SHELXL-97. Program Crystal Structure Refinement, University of Göttingen, Germany, 1997.
[7] J. Rodriguez-Carvajal, Physica B 192 (1993) 55.
[8] T. Roisnel, J. Rodriguez-Carvajal, Materials science forum, in: Proceedings of the European Powder Diffraction Conference (EPDIC7), 2000, p. 118.
[9] E. Parthe, L. Gelato, B. Chabot, M. Penzo, K. Cenzual, R. Gladyshevskii, TYPIX Standardized Data and Crystal Chemical Characterization of Inorganic Structure Types, Springer, Berlin, Heidelberg, 1994.
[10] DIAMOND. Release 3.0e, CRYSTAL IMPACT K. Brandenburg & M. Berndt GbR, Bonn, Germany, 2005.
[11] M.V. Bulanova, P.N. Zheltov, K.A. Meleshevich, P.A. Saltykov, G. Effenberg, J. Alloys Compd. 345 (2002) 110.
[12] P. Schobinger-Papamantellos, K.H.J. Buschow, J. Alloys Compd. 198 (1993) 47.
[13] H. Okamoto, J. Phase Equilib. Diff. 28 (2) (2007) 231.
[14] H. Langer, E. Wachtel, Z. Metallkd. 72 (1981) 769.
[15] R. Massara, P. Feschotte, J. Alloys Compd. 190 (2) (1993) 249.
[16] H. Okamoto, J. Phase Equilib. 12 (6) (1991) 700.
[17] T. Bretschneider, H.J. Schaller, Z. Metallkd. 81 (1990) 84.
[18] J.P. Kappler, M.J. Besnus, P. Lehmann, A. Meyer, J. Sereni, J. Less-Common Met. 111 (1–2) (1985) 261.
[19] J.R. Thomson, J. Less-Common Met. 13 (1967) 307.
[20] N. Kuwano, S. Higo, K. Yamamoto, K. Oki, T. Eguchi, Jpn. J. Appl. Phys. 24 (1985) L663.
[21] A. Palenzona, S. Cirafici, Thermochim. Acta 12 (1975) 267.
[22] A.V. Morozkin, Y.D. Seropegin, J. Alloys Compd. 237 (1–2) (1996) 124.
[23] C. Godart, L.C. Gupta, C.V. Tomy, S. Patil, R. Nagarajan, E. Beaurepaire, R. Vijayaraghavan, J.V. Yakhmi, Mater. Res. Bull. 23 (1988) 1781.
[24] J. Kitagawa, Y. Muro, N. Takeda, M. Ishikawa, J. Phys. Soc. Jpn. 66 (7) (1997) 2163.
[25] D. Rossi, R. Marazza, R. Ferro, J. Less-Common Met. 66 (2) (1979) 17.
[26] Y.M. Prots, W. Jeitschenko, M. Gerdes, B. Kuennen, Z. Anorg. Allg. Chem. 624 (1998) 1855.
[27] A.I. Tursina, A.V. Gribanov, Y.D. Seropegin, O.I. Bodak, J. Alloys Compd. 319 (2001) 145.
[28] J.M. Moreau, J. Le Roy, D. Paccard, Acta Crystallogr. 38 (1982) 2446.
[29] A.V. Gribanov, Y.D. Seropegin, O.I. Bodak, J. Alloys Compd. 204 (1994) L9.
[30] A.V. Gribanov, Y.D. Seropegin, O.L. Kubarev, L.G. Akselrud, O.I. Bodak, J. Alloys Compd. 317–318 (2001) 324.
[31] D.T. Adroja, B.D. Rainford, Physica B 230–232 (1997) 762.
[32] R. Mallik, E.V. Sampathkumaran, J. Magn. Magn. Mater. 164 (1–2) (1996) L13.
[33] B.I. Shapiev, O.L. Sologub, J.D. Seropegin, O.I. Bodak, P.S. Salamakha, J. Less-Common Met. 175 (1) (1991).
[34] T.B. Massalski (Ed.), Binary Alloy Phase Diagrams, second ed., ASM International, Materials Park, Ohio, USA,1990.
[35] P. Villars, L.D. Calvert (Eds.), Pearson's Handbook of Crystallographic Data for Intermetallic Phases, ASM International, Materials Park, Ohio, USA, 1991.
[36] B. Predel, in: W. Martienssen (Ed.), Landolt–Börnstein—Group IV Physical Chemistry, Springer, Berlin, 1993.
[37] I.R. Harris, G.V. Raynor, C.J. Winstanley, J. Less-Common Met. 12 (1) (1967) 69.
[38] C.D.W. Jones, R.A. Gordon, B.K. Cho, F.J. Disalvo, J.S. Kim, G.R. Stewart, Physica B: Condens. Matter 262 (3) (1999) 284.
[39] D. Rossi, R. Ferro, R. Marazza, J. Less-Common Met. 40 (3) (1975) 345.
[40] Y. Sakamoto, K. Takao, M. Ohmaki, J. Less-Common Met. 162 (2) (1990) 343.
[41] N. Kuwano, K. Umeo, K. Yamamoto, M. Itakura, K. Oki, J. Alloys Compd. 182 (1) (1992) 61.
[42] Z. Kang-Hou, C. Li-Li, Acta Chim. Sin. 47 (1989) 592.
[43] J.A. Wysocki, P.E. Duwez, Metall. Trans. 12A (1981) 1455.
[44] Z. Du, C. Guo, X. Yang, T. Liu, Intermetallics 14 (5) (2006) 560.
[45] C. Canali, L. Silvestri, G. Celotti, J. Appl. Phys. 50 (9) (1979) 5768.
[46] R. Marani, F. Nava, A. Rouault, R. Madar, J.P. Senateur, J. Phys.: Condens. Matter 1 (34) (1989) 5887.
[47] H. Pfisterer, K. Schubert, Die Naturwissenschaften 37 (5) (1950) 112.
[48] A. Szytuła, M. Hofmann, B. Penc, M. Slaski, S. Majumdar, E.V. Sampathkumar, A. Zygmunte, J. Magn. Magn. Mater. 202 (1999) 365.
[49] A.V. Gribanov, International Centre for Diffraction Data, PDF-54-0512 (2003).
[50] D. Huo, J. Sakurai, T. Kuwai, T. Mizushima, Y. Ishikawa, Phys. Rev. B 65 (2002) 144450/1.
[51] Y. Ishii, M. Kosaka, H. Abe, H. Kitazawa, G. Kido, Y. Uwatoko, J. Magn. Magn. Mater. 277 (1–2) (2004) 60.
[52] R. Ballestracci, Compt. Rend. Acad. Sci. Paris B282 (1976) 291.
[53] B.H. Grier, J.M. Lawrence, V. Murgai, R.D. Parks, Phys. Rev. B 29 (1984) 2664.
[54] A. Palenzona, S. Cirafici, F. Canepa, J. Less-Common Met. 135 (1987) 185.
[55] M.J. Besnus, A. Braghta, A. Meyer, Z. Physik B 83 (2) (1991) 207.
[56] J. Kitagawa, N. Takeda, M. Ishikawa, J. Alloys Compd. 256 (1997) 48.
[57] A.M. Strydom, A.P. Pikul, D. Kaczorowski, J. Alloys Compd. 351 (1–2) (2003) 54.